

# Functional imaging studies of cognition using $^{99m}\text{Tc}$ -HMPAO SPECT: empirical validation using the $n$ -back working memory paradigm

Catherine Ludwig · Christian Chicherio ·  
Luc Terraneo · Pierre Magistretti ·  
Anik de Ribaupierre · Daniel Slosman

Received: 16 March 2007 / Accepted: 2 October 2007 / Published online: 11 December 2007  
© Springer-Verlag 2007

## Abstract

**Purpose** Functional activation protocols are widely applied for the study of brain-cognition relations. Only few take advantage of the intrinsic characteristics of SPECT, particularly those allowing cognitive assessment outside of the camera, in settings close to the standard clinical or laboratory ones. The purpose of the study was to assess the feasibility of a split-dose activation protocol with  $^{99m}\text{Tc}$ -HMPAO using low irradiation dose.

**Materials and methods** A two-scans protocol was applied to 12 healthy young volunteers using 270 MBq of  $^{99m}\text{Tc}$ -HMPAO per scan, with each image associated to a particular experimental condition of the verbal  $n$ -back working memory task (0-back, 2-back). Subtraction method was used to identify regional brain activity related to the task.

**Results** Voxel-wise statistical analysis showed left lateralized activity associated with the 2-back task, compared to the 0-back task. Activated regions, mainly prefrontal and parietal, were similar to those observed in previous fMRI and  $^{15}\text{O}$ -PET studies.

**Conclusion** The results support the use of  $^{99m}\text{Tc}$ -HMPAO SPECT for the investigation of brain-cognition relations and demonstrate the feasibility of optimal quality images despite low radiopharmaceutical doses. The findings also acknowledge the use of HMPAO as a radioligand to capture neuro-energetic modulations linked to cognitive activity. They encourage extending the application of the described activation protocol to clinical populations.

**Keywords**  $^{99m}\text{Tc}$ -HMPAO SPECT · Brain imaging · Activation study · Working memory · Protocol validation

C. Ludwig (✉) · A. de Ribaupierre  
Center for Interdisciplinary Gerontology, University of Geneva,  
Geneva, Switzerland  
e-mail: Catherine.Ludwig@pse.unige.ch

C. Chicherio  
Center for Lifespan Psychology,  
Max Planck Institute for Human Development,  
Berlin, Germany

L. Terraneo  
Service of Nuclear Medicine, Geneva University Hospitals,  
Geneva, Switzerland

P. Magistretti  
Brain Mind Institute, EPFL,  
Lausanne, Switzerland

D. Slosman  
Nuclear Medicine Institute, Clinique Générale-Beaulieu,  
Geneva, Switzerland

## Introduction

In the past two decades, functional brain imaging has become a major tool to investigate the neural bases of cognition. The field of cognitive neuroscience has witnessed rapid growth following the introduction of water-labelled positron emission tomography ( $^{15}\text{O}$ -PET) and, more recently, functional magnetic resonance imaging (fMRI). Both techniques have major advantages, among them providing a true measure of brain metabolism (PET) and remarkably good spatial and temporal resolutions (fMRI). Furthermore, these techniques allow multiple repeats of various conditions, a fact that increases the accuracy of the data collected.

However, despite these major advantages, both PET and fMRI require the cognitive task to be performed inside the

scanner. The several drawbacks of this situation (uncomfortable supine position, noisy environment, limited “ecological” assessment), may affect the participant’s behaviour by causing interference with the ongoing cognitive activity [1]. Additionally, participants need to remain in the scanner throughout the whole experiment, which may be hard for individuals who, for whatever reason, have difficulty staying in a motion-free decubitus position for a long time.

By contrast, single photon emission computerized tomography (SPECT) using  $^{99m}\text{Tc}$ -HMPAO (*d,l*-hexamethyl propyleneamine oxime) or  $^{99m}\text{Tc}$ -ECD (*L,L*-ethylcysteinate dimer) allows dissociation of task administration and image acquisition. Cognitive activity occurs outside the scanner, and the time for which participants are required to remain in the scanner is substantially reduced, corresponding only to the duration of image acquisition. Hence, contrary to PET or fMRI, SPECT provides a means to measure brain regional metabolism associated with cognitive processes while keeping conditions close to standard laboratory ones.

Only few studies have taken advantage of SPECT for its use with healthy young adults [2–10], although they have provided encouraging support for the feasibility of activation protocols with  $^{99m}\text{Tc}$ -ECD or  $^{133}\text{Xe}$ . To our knowledge, however, only one cognitive activation study using  $^{99m}\text{Tc}$ -HMPAO has been reported with healthy young subjects [11]. Hence, there is a need to validate the use of this particular radiotracer in experiments devoted to investigate brain-cognition relations. Moreover, and given that HMPAO uptake is closely related to neuro-energetic mechanisms in the brain [12], it is undoubtedly an appropriate candidate to trace differential metabolic changes associated with cognitive activity. Another appealing advantage of  $^{99m}\text{Tc}$ -HMPAO SPECT is its application in the diagnosis of neurodegenerative diseases [13]. There is evidence showing that  $^{99m}\text{Tc}$ -HMPAO SPECT allows to discriminate between Alzheimer’s disease (AD) on the one hand, and frontotemporal dementia [14] or Lewy bodies disease [15, 16] on the other hand. More, and of greater interest to the present purpose, there is very recent evidence showing that  $^{99m}\text{Tc}$ -HMPAO SPECT allows to discriminate early dysfunction associated with AD, most particularly when the brain is under cognitive “stress”, as reached using cognitive activation [17, 18]. Thus, not only there is a need to validate the use of  $^{99m}\text{Tc}$ -HMPAO SPECT for activation studies in healthy young populations, but also to offer a protocol easily applicable in clinical settings for investigations of various states, among which normal and pathological aging.

Another challenge of the present study was to considerably reduce the recommended 555 MBq [7, 8] or 370 MBq [4, 5] of radioactivity to 270 MBq per scan, yet preserving the high quality of the images. We used a 1 to 1 dose ratio across scans as commonly applied in  $^{99m}\text{Tc}$  SPECT

activation studies [4, 5, 7, 8], although other methods have been proposed, such as increasing the second dose by a factor of approximately 2.0 [19, 20]. Notably, while the latter is meant to increase the signal to noise ratio, lowered by the pile-up effect inherent to the split-dose protocol, the former allows a larger reduction of the subject’s exposure to radioactivity. Moreover, images can be post-processed using proportional scaling to reliably grasp between-conditions differential activities [21], despite the pile-up effect (see the post-processing and statistical analyses section). For all these reasons, and because of particular radioprotection concerns, we favoured a 1 to 1 ratio procedure.

Finally, we addressed the feasibility of the activation protocol by convergent validity of the results. We used a cognitive activation task, the *n*-back, for which a large ensemble of comparable results has been already reported in the neuroimaging literature [22–26]. This task is currently one of the paradigms for which the most precise knowledge of the underlying functional architecture is available [27]. Replicating the findings reported both with  $^{15}\text{O}$ -PET and fMRI would support the validity and the feasibility of cognitive activation studies with low-dose  $^{99m}\text{Tc}$ -HMPAO SPECT.

## Materials and methods

**Subjects** The population consisted of 12 healthy young adults (10 women, 2 men), with an average age of 26.42 years (SD=2.57, range 23 to 31) and an educational level of 20.08 years (SD=1.98, range 17 to 24). All participants were right-handed (as assessed by the Oldfield-Edinburgh Inventory [28]) and fluent in French. None reported a history of medical, neurological or psychiatric disease. The participants were recruited in the university community by means of advertisements, and all signed written informed consent for participation. The experiment was approved by the ethics committees of the Geneva University Hospitals and of the Faculty of Psychology and Educational Sciences at the University of Geneva.

**Neuropsychological procedure** The verbal *n*-back task [26] was administered to the participants. The subjects were visually presented with series of letters (upper and lower case consonants), displayed one after the other at the centre of the computer screen. The 0-back condition, which served as a reference, consisted in deciding whether each stimulus corresponded to a specific target (letter “X”). The 2-back condition consisted in deciding whether each stimulus corresponded to the antepenultimate one in the sequence. In each condition, 6 blocks of 36 trials were built, for a total of 216 trials. The trial sequence was made up of a 500 ms

stimulus display followed by a 2,500 ms fixation point (see Fig. 1). One third of the items were selected as targets, randomly arranged in each block. Within each condition, block and trial order were maintained constant across participants. The 0-back was always provided before the 2-back. The task was computerized and built using E-Prime Software (Psychology Software Tools, Pittsburgh, PA, USA). The script was run on a Dell (Round Rock, TX, USA) personal computer provided with an E-Prime Serial Response Box device and a 15-in. monitor with 640×480 pixels resolution. For each trial, time and accuracy of responses were recorded online by the computer.

**Nuclear medicine procedure** Each of the two experimental conditions of the cognitive task was associated with a single full brain scan recording. A split-dose technique was applied to the participants using 270 MBq (7.3 mCi) of  $^{99m}\text{Tc}$ -HMPAO per scan.  $^{99m}\text{Tc}$ -HMPAO was prepared according to the recommendations of the manufacturer (Ceretec, Amersham, UK) and intravenously injected no longer than 20 min after preparation. Both tasks were performed in the scanning room but outside the scanner apparatus, providing settings close to laboratory conditions. The participants were invited to sit comfortably in front of the computer, with the left arm lying onto a small table. An intravenous butterfly catheter was placed in the elbow fold in preparation for subsequent radiopharmaceutical intravenous injection. The task instructions for the 0-back condition were provided, and the six experimental blocks were administered. The tracer was injected at the beginning of the third block. Due to the rapid first-pass extraction of  $^{99m}\text{Tc}$ -HMPAO [29], brain images reflect the average activity that was labelled during the third and fourth blocks. At the end of the task, the participants were required to rest during the washout period (at least 20 min, see Table 1) before being placed in the scanner in a decubitus position. Image acquisition lasted 30 min. The same procedure was applied for the acquisition of the second brain image

associated with the 2-back condition. The interval between the end of the first scan and the acquisition of the second one was approximately 50 min. It is worth pointing out that inherent to the split-dose single day protocol is contamination of the second scan by the remaining activity of the first one [5, 6]. However, it has been argued that the pile-up does not prevent the conduction of neurofunctional activation studies [4, 5, 21], particularly if post-processing involves proportional scaling procedures. Indeed, the latter allows statistical control for global variations in the signal across scans and conditions [21].

**Quality control procedure** For each scan, quality controls concerned the dose preparation, the effective dose administered to the subjects, the injection/acquisition delay and the total counts obtained in the reconstructed images. For each dose administered, the syringe radioactive content, in MBq, was measured by means of standard laboratory procedures. Pre- and post-injection counts were subsequently acquired by recording the radioactivity of the source using the Toshiba-GCA gamma camera, calibrated on 140 KeV. Acquisition was performed in a fixed mode for 5 min. A region of interest (ROI) was manually drawn around radioactive foci. To complete quality control measures, the time between injection and acquisition was recorded.

**Acquisition protocol** For both scans, SPECT acquisition was performed at least 20 min after i.v. injection using a triple head Toshiba GCA-9300 gamma camera (Toshiba Medical Systems, Tokyo, Japan) with a fan beam high resolution collimation. Data were acquired on a 128×128 matrix, with a 360° rotation angle and a step-and-shoot mode (6° step angle and 90 s rotation time), providing 60 projections.

Given that our aim was to develop a protocol that could be easily implemented in clinical settings, and despite the recent development of alternative methods [19], image processing was conducted by means of methods currently available in most commercially distributed processing

**Fig. 1** Schematic representation of the trial sequences used in the 0-back condition (*left panel*) and in the 2-back condition (*right panel*)

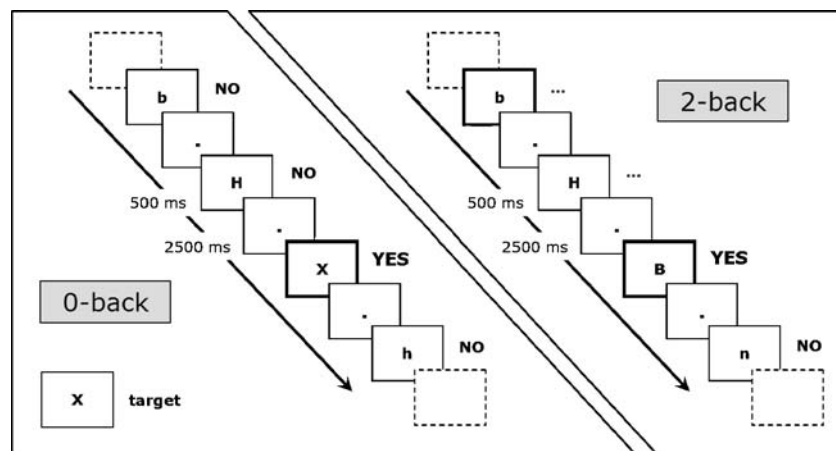


**Table 1** Quality control values, by scan and participant

Subjects	Scan 1				Scan 2			
	Activity (MBq)	% cnt red.	Time (min)	Scan Tcounts	Activity (MBq)	% cnt red.	Time (min)	Scan Tcounts
1	272.70	86.52	25	2,765.5	270.80	94.88	23	5,596.2
2	270.90	95.91	22	3,344.9	271.10	97.40	22	6,539.5
3	263.40	95.97	22	3,326.7	277.20	95.91	20	6,331.8
4	276.50	97.18	24	4,587.3	277.50	99.47	28	9,635.5
5	277.10	96.96	20	3,817.8	270.50	95.48	20	6,928.9
6	272.90	89.79	24	2,758.1	276.50	96.42	21	5,727.6
7	267.30	95.33	23	3,499.0	278.30	96.17	20	7,478.4
8	273.00	96.26	21	4,031.6	270.80	94.87	20	8,406.3
9	271.90	96.73	20	3,403.5	277.60	95.13	25	6,638.7
10	271.00	99.18	20	4,242.8	271.00	99.13	26	7,684.9
11	265.70	96.88	22	3,015.4	266.30	99.27	30	5,305.7
12	272.90	96.34	25	3,192.1	272.50	96.69	27	6,598.6
M	271.28	95.25	22	3,498.7	273.34	96.74	24	6,906.0
Sd	4.06	3.52	2	572.1	3.89	1.71	4	1,240.6

Counts are expressed in  $10^{-4}$

*Activity*, Dose activity as measured by standard laboratory procedures; *% cnt red.*, percentage reduction of counts measured in syringe after injection; *Time*, time elapsed between injection and acquisition; *Scan Tcounts*, total number of counts in brain scan

software. These methods are routinely performed, and have been discussed in the literature for SPECT activation protocols [4, 5, 7, 8]. Thus, scatter correction was performed using the TEW method [30], with 20% set around the 140 KeV peak, and an additional 7% in the upper and lower sides of the main window. Images were reconstructed in a  $128 \times 128$  matrix. Attenuation correction was done by filtered back projection (Sorenson method) using a Butterworth filter of 8.0.16 for the main window and of 8.0.09 for the sub-windows. The attenuation correction map was automatically drawn with a contour set at 5%, and an attenuation coefficient set to  $0.09 \text{ cm}^{-1}$ . Image reconstructions used a Shepp & Logan filter in the axial, coronal and sagittal planes with a slice thickness of 1 pixel. Voxel size was  $3.44 \text{ mm}^3$ . Examples of reconstructed images are provided in Fig. 2.

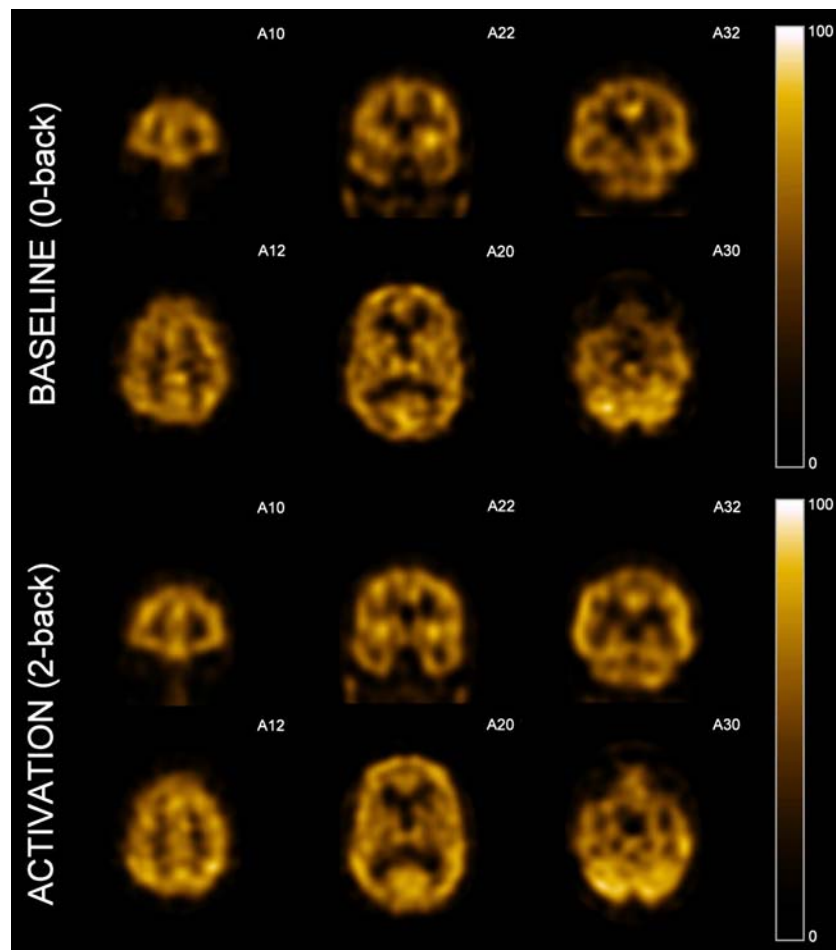
*Post-processing and statistical analyses* The original Toshiba raw data files were converted into Analyze format using MedX software (Sensor Systems, Sterling, VA, USA). By means of SPM2 (Department of Cognitive Neurology, Institute of Neurology, London, UK) implemented in MatLab 6.5 (Math-Works, Sherborn, MA, USA), the different images of a participant were realigned, creating a mean volume of resliced scans. Images were further normalized into the Talairach and Tournoux stereotaxic space [31], using the mean images to obtain the parameters' values and applying to the resliced images a trilinear interpolation with eight non-linear iterations. Co-registration, realignment and normalization were conducted to match each scan onto a common reference space, hence minimizing individual differences in anatomy and allowing

subsequent voxel-wise analyses. Finally, images were smoothed using a Gaussian filter of  $10 \times 10 \times 12 \text{ mm}^3$  at full width half maximum (FWHM). Subtraction method was applied to count densities on a voxel-by-voxel basis to determine brain areas of significantly increased or decreased activity. Differences in global activity between scans were removed by scaling the activity in each voxel proportional to the averaged global activity [21]. Grand mean values were computed using a grey matter threshold of 0.5. This proportional scaling procedure not only allows statistical control for differences in global scan activity and cross-scan activity accumulation, but also increases the sensitivity in detecting small variation in the signal associated with the experimental conditions. Finally, to obtain a more readily comprehensible unit of activity, the corrected values were adjusted around a grand mean of  $50 \text{ ml/min/100 g}$ , corresponding to the approximated average blood flow as measured by  $^{15}\text{O}$ -PET. The effect of task conditions (2-back vs 0-back) on the count density at each voxel was estimated using a general linear model, wherein the changes in global counts are considered as a covariate. Linear contrasts of the means across conditions were used on a voxel-by-voxel basis using  $t$  statistics. The resulting sets of  $t$  values constituted statistical parametric maps  $\text{SPM}(t)$ , that were subsequently transformed to unit normal distribution  $\text{SPM}(Z)$  maps.

## Results

*Quality control* Quality control values are reported in Table 1. Of particular interest is the low inter-subject

**Fig. 2** Example of raw SPECT images of the 0-back and 2-back conditions in the coronal and axial planes (images are displayed according to the radiological convention)



variability in (a) the radioactivity values collected by means of laboratory procedures, (b) the percentage reduction in counts post-injection and (c) the time interval between injection and acquisition. Furthermore, these values measured for scan 1 and scan 2 were not significantly different, as assessed by paired-samples *t* tests conducted on each variable separately. All analyses yield *p* values larger than 0.15. Finally, it is important to stress that all images acquired were of good quality (see Fig. 2 as an example), and all were taken into account for further analysis.

**Imaging data** Inferential statistics on brain imaging data were conducted using SPM2 (Department of Cognitive Neurology, Institute of Neurology, London, UK). A multi-subjects, condition, and covariates design was applied, with two conditions (0-back, 2-back), but no behavioural covariates. The analysis was performed without correction for multiple comparisons, using a *p* value threshold of  $p=0.001$  and a cluster of at least 20 voxels for the peaks to be considered. Detailed results are reported in Table 2. Given that the sample included two men and ten women, and that controversies exist in the literature with respect to gender differences [32, 33], we individually compared each man's

pattern of activity to the average pattern found in the group of women using the method proposed by Signorini [34]. No significant differences were found. Therefore, we pooled all scans together to increase statistical power and report the findings relative to the complete sample of 12 participants. Of direct interest to the present purpose is the increased activity specifically associated with the 2-back condition [for the corresponding SPM(*Z*) maps, see Fig. 3]. The peaks occur in an ensemble of areas involving, on the left side, the frontopolar (BA10) and dorsolateral (BA46) regions of the prefrontal cortex, the frontal eye field (BA8), and the left inferior parietal lobule (BA40). Additionally to these left-sided foci, areas of the right hemisphere demonstrated specific activations during the 2-back task; these include the orbitofrontal (BA11) and frontopolar (BA10) cortices as well as the somatosensory and motor primary regions (BA3/4) and the superior parietal lobule (BA7). Finally, increased bilateral activity was found in the visual association areas, mainly involving the cuneus (BA18).

**Behavioural data** Analysis of the behavioural data was performed on the median response times, computed only on correct responses and on the proportion of correct

**Table 2** Peak coordinates (*x, y, z*) of significant condition effects, with associated *Z* value and anatomical areas

<i>x</i>	<i>y</i>	<i>z</i>	Cluster <i>p</i> (unc)	voxel <i>Z</i>	Voxel <i>p</i> (unc)	BA	Anatomical area
-22	38	40	0.003	4.56	0.000	BA8	Left superior frontal gyrus
-22	30	48		3.89	0.000	BA8	Left superior frontal gyrus
-30	54	0	0.002	4.42	0.000	BA10	Left superior frontal gyrus
-28	50	20		3.36	0.000	BA10	Left middle frontal gyrus
28	-30	68	0.045	4.09	0.000	BA3	Right post-central gyrus
36	-22	60		3.84	0.000	BA4	Right pre-central gyrus
-18	-92	12	0.006	3.96	0.000	BA18	Left cuneus
28	-52	48	0.021	3.89	0.000	BA7	Right superior parietal lobule
-42	-56	40	0.028	3.81	0.000	BA40	Left inferior parietal lobule
24	52	-8	0.009	3.68	0.000	BA10	Right middle frontal gyrus
36	42	-8		3.17	0.001	BA11	Right middle frontal gyrus
28	-80	8	0.085	3.53	0.000	BA18	Right cuneus
30	-80	20		3.21	0.001	BA19	Right cuneus
-44	32	16	0.076	3.49	0.000	BA46	Left middle frontal gyrus
52	-42	-4	0.045	3.45	0.000	BA37	Right middle temporal lobe

*p*(unc), *p* values uncorrected for multiple comparisons; BA, Brodmann's area

responses. Scores were averaged for blocks 1 and 2, blocks 3 and 4 and blocks 5 and 6, corresponding to the events occurring before injection and tracer uptake, during uptake and after uptake, respectively. Descriptive statistics by Period (before, during, after) and Condition (0-back, 2-back) are graphically displayed in Fig. 4.

Inferential statistics were conducted using a  $2 \times 3$  ANOVA design, with the Condition (0-back, 2-back) and the Period (before, during, after uptake) as repeated measures. With respect to the median response times, results revealed a significant main effect of Condition  $F(1,11)=22.11$ ,  $p<.001$ ,  $\eta_p^2=0.67$ , but the main effect of Period,  $F(2,22)=0.64$ ,  $p=0.54$ , and the Condition $\times$ Period interaction,  $F(2,22)=0.80$ ,  $p=0.46$ , were not significant. As concerns the proportion of correct responses, a similar pattern was observed with a significant main effect of Condition,  $F(1,11)=7.28$ ,  $p<.05$ ,  $\eta_p^2=0.40$ , but no significant main effect of Period,  $F(2,22)=2.04$ ,  $p=0.15$ , and no significant Condition $\times$ Period interaction,  $F(2,22)=1.10$ ,  $p=0.35$ . Altogether, these results are in line with previous findings reported in the literature [35, 36] and support the hypothesis of an increase in cognitive demand associated with the 2-back condition, as compared to the 0-back. Indeed, in the former, participants take more time to

respond and demonstrate lower accuracy. It is also worth pointing out that performance remains stable across the three time periods, with similar patterns in both tasks.

## Discussion

Findings from the present experiment using a  $^{99m}\text{Tc}$ -HMPAO SPECT split-dose activation protocol are rather encouraging with respect to the two goals pursued. First, from a technical and methodological point of view, these results were supportive of the use of  $^{99m}\text{Tc}$ -HMPAO as a radiotracer labelling differences in metabolism during cognitive activation and of the possibility of collecting good quality brain images despite relatively low doses of radiopharmaceuticals. Second, results regarding the localizations of brain activations during a verbal working memory task were in good agreement with those reported in the literature. Convergent validity was adequately demonstrated, hence providing additional support for the feasibility of cognitive activation studies with  $^{99m}\text{Tc}$ -HMPAO SPECT.

Concerning the behavioural data, performance was significantly lower in the 2-back condition than in the

**Fig. 3** SPM(*Z*) maps for the 2-back minus 0-back contrast, displayed according to the neurological convention

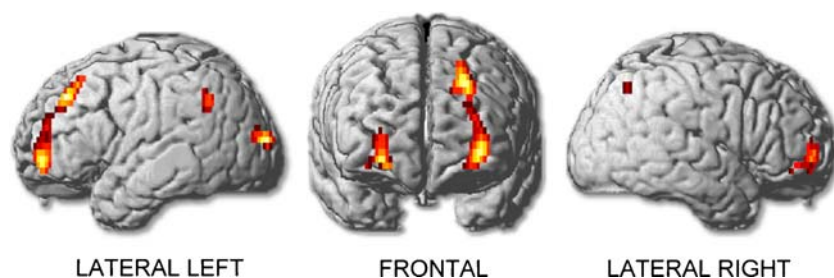
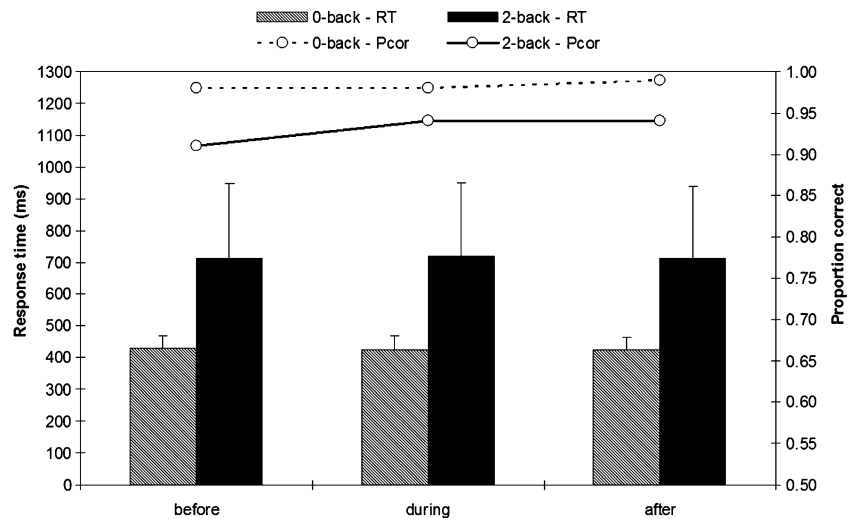


**Fig. 4** Behavioural results: median response times (RT, bars) and proportion of correct responses (Pcor, lines) before, during and after uptake, for the 0-back and the 2-back conditions



0-back one, which replicated previous findings [35, 36] and supported the assumption that the 2-back was more demanding in processing resources from the executive component of working memory [23, 24]. Involvement of working memory was further supported by brain imaging results, which revealed that the 2-back condition was associated with increased activity in left prefrontal areas (extending to the right hemisphere), the left parietal lobule (BA40) and bilateral occipital areas. As pointed out by Owen et al. [27] in a recent meta-analysis of functional imaging studies using the *n*-back task, the fronto-parietal network involvement in the 2-back task is currently largely undisputed. The fact that the major brain areas reported in the literature using  $^{15}\text{O}$ -PET or fMRI were also found in the present study strongly supports the validity of the measures acquired with  $^{99\text{m}}\text{Tc}$ -HMPAO SPECT, and provides good evidence for a reliable application of the present protocol for brain imaging experiments.

Two major issues need further discussion: the advantages vs. limitations of SPECT for cognitive activation studies, and the choice of HMPAO over ECD as ligand to assess brain energy metabolism. Although widely applied in clinical routine, SPECT has been rarely used for activation studies in the field of cognitive neurosciences compared to fMRI, or even  $^{15}\text{O}$ -PET. Both latter techniques benefit from almost real-time imaging of the brain, allow repetitions of intra-individual scan acquisitions and offer a precise spatial resolution. However, they require a fairly rigid experimental set-up, and the participant has to perform the cognitive test within the scanner and remain in a decubitus position throughout the whole experiment. Such technical and environmental constraints not only restrict comfort for the participant but also prevent assessment of individuals who cannot remain still in the scanner for a long time. Even more important is the non-negligible disruptive impact of the fMRI noisy environment on the cognitive

processing under investigation [1]. This effect may possibly compromise between-group comparisons, given that various pathological states, or even advancing age, are related to differences in the susceptibility to interfering sources of information [37]. Hence, with respect to this particular issue, SPECT undoubtedly demonstrates large advantages by allowing cognitive assessment to be conducted outside the scanner. Another major advantage of the protocol we propose is its potential application in clinical populations, more specifically in cases of neurodegenerative diseases. Indeed, there is increasing evidence that  $^{99\text{m}}\text{Tc}$ -HMPAO SPECT permits discrimination of functional specificities across different types of dementias [14, 15] even before abnormalities are reported with structural imaging. Of additional interest is very recent evidence demonstrating that early dysfunction found in Alzheimer's disease is best apprehended during cognitive activation as compared to rest [17, 18]. Hence, although  $^{99\text{m}}\text{Tc}$ -HMPAO SPECT might not be the most appropriate technique to investigate the neurofunctional bases of cognition in young healthy populations, its application might become particularly relevant for the study of normal and pathological aging, and the early detection of functional deficits associated with neurodegenerative diseases.

SPECT does have several limitations. Among these are the small number of intra-individual brain recordings and the limited ability, due to its moderate resolution, to detect signal differences between individuals. Although these limitations need to be recognized, encouraging findings already support the use of SPECT for activation studies [4, 5, 7, 8], which should not be dismissed. Moreover, previous studies have demonstrated that the moderate resolution of SPECT does not prevent applying voxel-based analyses to SPECT images, and that approaches such as statistical parametric mapping (SPM) can adequately be employed [2, 21], even with rather small samples [38]. The

findings from the present study also confirm the feasibility of activation protocols with SPECT, despite intrinsic limitations.

The present work is also one of the first contributions providing a clear demonstration that SPECT can be successfully performed with  $^{99m}\text{Tc}$ -HMPAO in activation experiments. To date, at least in healthy young populations, most comparable studies exclusively used  $^{99m}\text{Tc}$ -ECD, probably because ECD has long been considered to reflect regional cerebral blood flow (rCBF) better than  $^{99m}\text{Tc}$ -HMPAO. Recent work, however, has pointed out a cardinal linkage between HMPAO retention dynamics and neuroenergetic mechanisms in the brain [13, 39]. More specifically, HMPAO is prominently retained in astrocytes [12], a cell type for which a central role in coupling neuronal activity to glucose utilization [40] and blood flow [41] has been demonstrated. Targeting this particular metabolic dynamics supports favoring HMPAO over ECD to precisely trace metabolic changes related to cognitive activity, and particularly those associated with memory [42, 43]. In this vein, and as already underlined earlier, the use of HMPAO may be very helpful in tracing dysfunctions associated with pathological processes that affect glial cells, such as alterations of astrocyte function in degenerative diseases [44, 45], or changes in microglia occurring in the course of normal aging [46].

The present study provides substantial support for the feasibility of a split-dose  $^{99m}\text{Tc}$ -HMPAO SPECT activation protocol and reveals its ability to identify brain regions involved in cognitive activity. Our findings further warrant the use of HMPAO as a radioligand. Considering the emerging role of neuron–astrocyte interactions in coupling synaptic activity with metabolic and vascular responses [47], HMPAO may be better suited than ECD to capture neuroenergetic modulations associated with cognitive activity. Thus,  $^{99m}\text{Tc}$ -HMPAO SPECT activation protocols may attract increasing interest not only in the study of neurofunctional bases of cognition, but also, and most importantly, in further investigations of neuro-energetic dysfunctions in normal and pathological aging. Finally, the results broadly support performing brain-imaging experiments in settings close to standard clinical ones and associating low irradiation with high-quality images. In conclusion, this empirical validation study has shown that functional imaging studies of cognition using  $^{99m}\text{Tc}$ -HMPAO SPECT are both technically and methodologically feasible.

**Acknowledgement** The authors wish to thank the medical, technical and laboratory staff of the Service of Nuclear Medicine of Geneva University Hospitals who actively participated in the data collection. This work was supported by the Swiss National Research Foundation grants no. 1153-067087.01 and no. BPG E1 112883. The experiment complies with the current laws of Switzerland inclusive of ethics approval.

## References

- Gutchess AH, Park DC. fMRI environment can impair memory performance in young and elderly adults. *Brain Res* 2006;1099:133–40.
- Lahorte P, Vandenberghe S, Van laere K, Audenaert K, Lemahieu I, Dierckx RA. Assessing the performance of SPM analyses of SPECT neuroactivation studies. *Neuroimage* 2000;12:757–64.
- Montaldi D, Mayes AR. The neuroactivation of cognitive processes investigated with SPECT. *Behav Neuropsychiatry* 2000;12:53–7.
- Audenaert K, Brans B, van Laere K, Lahorte P, Versijpt J, van Heeringen K, et al. Verbal fluency as a prefrontal activation probe: a validation study using  $^{99m}\text{Tc}$ -ECD brain SPET. *Eur J Nucl Med* 2000;27:1800–808.
- Audenaert K, Lahorte P, Brans B, van Laere K, Goethals I, van Heeringen K, et al. The classical stroop interference task as a prefrontal activation probe: a validation study using  $^{99m}\text{Tc}$ -ECD brain SPECT. *Nucl Med Commun* 2001;22:135–43.
- Audenaert K, Goethals I, van Laere K, Lahorte P, Brans B, Versijpt J, et al. SPECT neuropsychological activation procedure with the Verbal Fluency Test in attempted suicide patients. *Nucl Med Commun* 2002;23:907–16.
- Goethals I, Audenaert K, Jacobs F, Van de Wiele C, Vermeir G, Vandierendonck A, et al. Toward clinical application of neuropsychological activation probes with SPECT: a spatial working memory task. *J Nucl Med* 2002;43:1426–31.
- Goethals I, Audenaert K, Jacobs F, Van de Wiele C, Pyck H, Ham H, et al. Application of a neuropsychological activation probe with SPECT: the ‘Tower of London’ task in healthy volunteers. *Nucl Med Commun* 2004;25:177–2.
- Cardebat D, Démonet J-F, Viillard G, Faure S, Puel M, Celsis P. Brain functional profiles in formal and semantic fluency tasks: A SPECT study in normals. *Brain Lang* 1996;52:305–13.
- Démonet J-F, Celsis P, Nespoulous J-L, Viillard G, Marc-Vergnes J-P, Rascol A. Cerebral blood flow correlates of word monitoring in sentences: Influence of semantic incoherence. A SPECT study in normals. *Neuropsychologia* 1992;30:1–11.
- Montaldi D, Mayes AR, Barnes A, Pirie H, Hadley DM, Patterson J, et al. Associative encoding of pictures activates the medial temporal lobes. *Hum Brain Mapp* 1998;6:85–104.
- Zerarka S, Pellerin L, Slosman DO and Magistretti PJ. Astrocytes as a predominant cellular site of ( $^{99m}\text{Tc}$ )-HMPAO retention. *J Cereb Blood Flow Metab* 2001;21:456–68.
- Magistretti PJ, Pellerin L. Cellular mechanisms of brain energy metabolism and their relevance to functional brain imaging. *Philos Trans R Soc Lond B Biol Sci* 1999;354:1155–63.
- Varrone A, Pappatà S, Caracò C, Soricelli A, Milan G, Quarantelli M, et al. Voxel-based comparison of rCBF SPET images in frontotemporal dementia and Alzheimer’s disease highlights the involvement of different cortical networks. *Eur J Nucl Med Mol Imaging* 2002;29:1447–54.
- Colloby SJ, Fenwick JD, Williams ED, Paling SM, Lobotesis K, Ballard C, et al. A comparison of ( $^{99m}\text{Tc}$ )-HMPAO SPET changes in dementia with Lewy bodies and Alzheimer’s disease using statistical parametric mapping. *Eur J Nucl Med Mol Imaging* 2002;29:615–22.
- Kemp PM, Hoffmann SA, Holmes C, Bolt L, Ward T, Holmes RB, et al. The contribution of statistical parametric mapping in the assessment of precuneal and medial temporal lobe perfusion by  $^{99m}\text{Tc}$ -HMPAO SPECT in mild Alzheimer’s and Lewy body dementia. *Nucl Med Commun* 2005;26:1099–106.
- Sundström T, Elgh E, Larsson A, Näsman B, Nyberg L, Riklund KA. Memory-provoked rCBF-SPECT as a diagnostic tool in Alzheimer’s disease? *Eur J Nucl Med Mol Imaging* 2006;33:73–80.
- Elgh E, Sundström T, Näsman B, Ahlström R, Nyberg L. Memory functions and rCBF ( $^{99m}\text{Tc}$ )-HMPAO SPET: developing diag-



- nostics in Alzheimer's disease. *Eur J Nucl Med Mol Imaging* 2002;29:1140–48.
19. Yokoi T, Shinohara H, Takaki A. Improvement of signal-to-noise ratio using iterative reconstruction in a 99m Tc-ECD split-dose injection protocol. *Eur J Nucl Med Mol Imaging* 2003;30:1125–33.
  20. Shedlack KJ, Hunter R, Wyper D, McLuskie R, Fink G, Goodwin GM. The pattern of cerebral activity underlying verbal fluency shown by split-dose single photon emission tomography (SPET or SPECT) in normal volunteers. *Psychol Med* 1991;21:687–96.
  21. Acton PD, Friston KJ. Statistical parametric mapping in functional neuroimaging: Beyond PET and fMRI activation studies. *Eur J Nucl Med* 1998;25:663–67.
  22. Awh E, Jonides J, Smith EE, Schumacher EH, Koeppel RA, Katz S. Dissociation of storage and rehearsal in verbal working memory: Evidence from Positron Emission Tomography. *Psychol Sci* 1996;7:25–31.
  23. Smith EE, Jonides J. Neuroimaging analyses of human working memory. *Proc Natl Acad Sci USA* 1998;95:12061–8.
  24. Smith EE, Jonides J. Working memory: A view from neuroimaging. *Cognit Psychol* 1997;33:5–42.
  25. Cohen JD, Forman SD, Braver TS, Casey BJ, Servan-Schreiber D, Noll DC. Activation of the prefrontal cortex in a nonspatial working memory task with functional MRI. *Hum Brain Mapp* 1994;1:293–304.
  26. Braver TS, Cohen JD, Nystrom LE, Jonides J, Smith EE, Noll DC. A parametric study of prefrontal cortex involvement in human working memory. *Neuroimage* 1997;5:49–62.
  27. Owen AM, McMillan KM, Laird AR, Bullmore E. N-Back working memory paradigm: A meta-analysis of normative functional neuroimaging studies. *Hum Brain Mapp* 2005;25:46–59.
  28. Oldfield RC. The assessment and analysis of handedness: The Edinburgh Inventory. *Neuropsychologia* 1971;9:97–113.
  29. Neirinckx RD, Burke JF, Harrison RC, Forster AM, Andersen AR, Lassen NA. The retention mechanism of technetium-99m-HM-PAO: intracellular reaction with glutathione. *J Cereb Blood Flow Metab* 1988;8:S4–S12.
  30. Ichihara T, Ogawa K, Motomura N, Kubo A, Hashimoto S. Compton scatter compensation using the triple-energy window method for single- and dual-isotope SPECT. *J Nucl Med* 1993;34:2216–21.
  31. Talairach J, Tournoux P. Co-planar atlas of the human brain. New York: Thieme Medical; 1988.
  32. Bell EC, Willson MC, Wilman AH, Dave S, Silverstone PH. Males and females differ in brain activation during cognitive tasks. *Neuroimage* 2006;30:529–38.
  33. Haut KM, Barch DM. Sex influences on material-sensitive functional lateralization in working and episodic memory: men and women are not all that different. *Neuroimage* 2006;32:411–22.
  34. Signorini M, Paulesu E, Friston KJ, Perani D, Colleluori A, Lucignani G, et al. Rapid assessment of regional cerebral metabolic abnormalities in single subjects with quantitative and nonquantitative [18F]FDG PET: A clinical validation of Statistical Parametric Mapping. *Neuroimage* 1999;9:63–80.
  35. Callicott JH, Mattay VS, Bertolino A, Finn K, Coppola R, Frank JA, et al. Physiological characteristics of capacity constraints in working memory as revealed by functional MRI. *Cereb Cortex* 1999;9:20–26.
  36. Jansma JM, Ramsey NF, Coppola R, Kahn RS. Specific versus nonspecific brain activity in a parametric N-back task. *Neuroimage* 2000;12:688–97.
  37. Dempster FN, Brainerd CJ. Interference and inhibition in cognition. San Diego, CA, USA: Academic; 1995.
  38. Tien AY, Schlaepfer TE, Orr W, Pearlson GD. SPECT brain blood flow changes with continuous ligand infusion during previously learned WCST performance. *Psych Res* 1998;82:47–52.
  39. Jacquier-Sarlin MR, Polla BS, Slosman DO. Oxido-reductive state: The major determinant for cellular retention of Technetium-99m-HMPAO. *J Nucl Med* 1996;37:1413–16.
  40. Tzacopoulos M, Magistretti PJ. Metabolic coupling between glia and neurons. *J Neurosci* 1996;16:877–85.
  41. Zonta M, Angulo MC, Gobbo S, Rosengarten B, Hossmann KA, Pozzan T, et al. Neuron-to-astrocyte signaling is central to the dynamic control of brain microcirculation. *Nat Neurosci* 2003;6:43–50.
  42. Caudle RM. Memory in astrocytes: a hypothesis. *Theor Biol Med Model* 2006;3:2.
  43. Jourdain P, Bergersen LH, Bhaukaurally K, Bezzi P, Santello M, Domercq M, et al. Glutamate exocytosis from astrocytes controls synaptic strength. *Nat Neurosci* 2007;10:331–39.
  44. Slosman DO, Ludwig C, Zerarka S, Pellerin L, Chicherio C, de Ribaupierre A, et al. Brain energy metabolism in Alzheimer's disease: 99mTc-HMPAO SPECT imaging during verbal fluency and role of astrocytes in the cellular mechanism of 99mTc-HMPAO retention. *Brain Res Rev* 2001;36:230–40.
  45. Beal MF. Mitochondria take center stage in aging and neurodegeneration. *Ann Neurol* 2005;58:495–505.
  46. Conde JR, Streit WJ. Microglia in the aging brain. *J Neuropathol Exp Neurol* 2006;65:199–203.
  47. Magistretti PJ, Pellerin L, Rothman DL, Shulman RG. Energy on demand. *Science* 1999;283:496–97.